Reading the Early Signs

Hinz, L.

2020

document version
Publisher's PDF, also known as Version of record

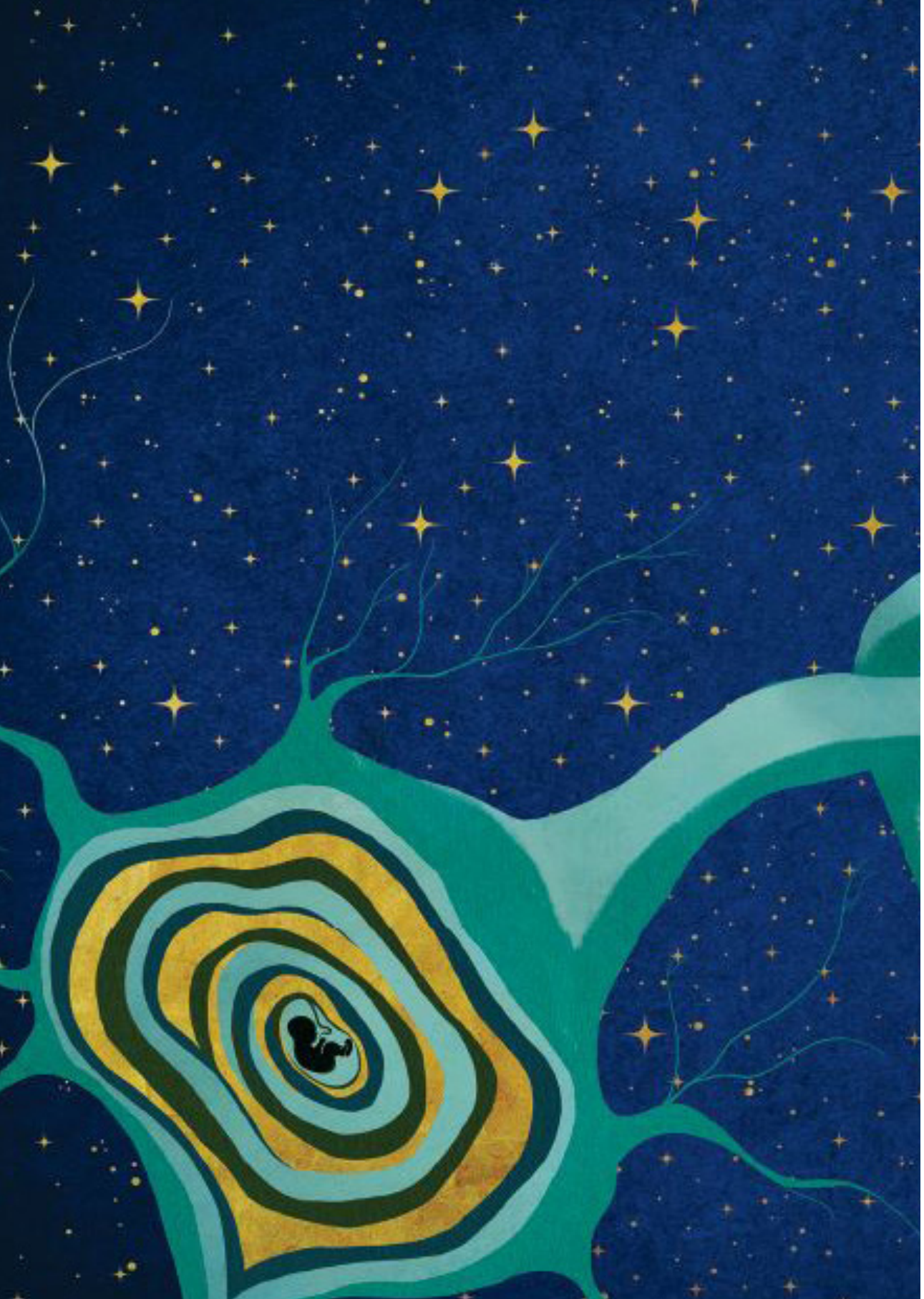

4

LACK OF MECP2 IN CORTICAL NEURONS FROM RETT SYNDROME PATIENTS CAUSES ALTERATION IN NEURONAL NETWORK DEVELOPMENT

Lisa Hinz[1], Johny Pires[2], Rhiannon Meredith[2], Danielle Posthuma[1,3], Vivi M. Heine[1,3,*]

[1]*Department of Complex Trait Genetics, Center for Neurogenomics and Cognitive Research, Amsterdam Neuroscience, Vrije Universiteit, Amsterdam, The Netherlands.*

[2]*Department of Integrative Neurophysiology, Center for Neurogenomics and Cognitive Research, Amsterdam Neuroscience, Vrije Universiteit, Amsterdam, The Netherlands.*

[3]*Department of Child Psychiatry, VU University Medical Center, Amsterdam Neuroscience, Amsterdam, The Netherlands.*

ABSTRACT

Rett Syndrome, a neurodevelopmental disorder often caused by mutations in the MECP2 gene, leads to symptoms such as autism-like and stereotypic behaviour, mental impairment, motor disabilities and severe seizures. First clinical symptoms are observed between 6 to 18 months of age, although brain abnormalities are expected to set at earlier stages. At a cellular level different studies showed that neurons with MECP2 mutations display an immature phenotype with decreased size and neurite outgrowth and show impaired functionality and reduced spontaneous activity. To investigate the cause of impaired functionality and early network developmental delay in RTT neurons, we evaluated the critical period of a developmentally restricted activity, spontaneous synchronous network activity (SSA). SSA is highly related to the induction of the GABAergic shift in certain brain areas, network development, neuronal maturation and synaptic pruning. Alterations in its critical period has been already associated with other neurodevelopmental disorders such as Autism Spectrum Disorders, Angelmann Syndrome and Fragile X Syndrome.

To investigate SSA alterations during a critical period in RTT, we used an iPSC-derived mixed population of inhibitory and excitatory cortical neurons from RTT patients and studied them over an early developmental period *in vitro*. SSA presence was evaluated using 2-photon calcium (Ca^{2+})-imaging by loading the cells with Ca^{2+}-sensitive dyes. With this approach we confirmed immaturity of RTT neurons due to decreased neurite outgrowth. Furthermore, we observed a delay of SSA appearance in RTT neurons and a reduced spiking frequency. Due to the altered SSA appearance, our results suggest a disturbance in neuronal network development, which consequently leads to an altered connectivity and an impaired balance of inhibition and excitation. Therefore, we hypothesize that the observed delay of SSA appearance in RTT neurons, leads to an impaired synaptogenesis and a delayed neuronal network development.

INTRODUCTION

Rett Syndrome (RTT) is a neurodevelopmental disorder typically presenting symptomatic onset between 6 to 18 months of age. It is associated with autistic behaviour, mental impairment, motor and breathing abnormalities and severe seizures. Classical RTT is caused by dominant mutations in the *MECP2* gene.[1–4] Given that *MECP2* is located on the X-Chromosome, RTT mainly affects females with a prevalence of 1:100,00. As a methyl CpG binding protein, MeCP2 is involved in gene regulation of hundreds of downstream target genes, what makes the identification of exact disease mechanisms difficult.[5] However, the neuronal phenotype of RTT is well studied. In *post mortem* brain tissue and mouse models, RTT neurons present as underdeveloped and immature with smaller soma, decreased neurite length and reduced numbers of synapses.[2,6,7] Besides the phenotypic alterations, researchers also identified a functional phenotype in RTT mouse models. Here, they found a reduction in spontaneous synaptic activity and a decrease in the number of glutamatergic synapses.[6,7] Also, impairment of Long-Term Potentiation (LTP) and seizures were observed in these mice, indicating disturbance of E/I balance.[8–10] A more recent study investigated alterations during the time point of birth and shortly after. They detected alterations in E/I balance and LTP impairment in RTT mice, caused by an insufficient shift of GABA from being excitatory to inhibitory.[11] As in humans the GABAergic shift is a pre-natal developmental process, translation to human patients is rather difficult.[12] However, the implementation of induced pluripotent stem cells (iPSCs) and iPSC-derived disease models provided remedy and helped to translate early developmental processes from a mouse to human model system. As iPSCs differentiation is capable to partly mimic development *in vivo*, the development of neurons can be observed over time and alterations within this process can be detected.[13] Therefore, the investigation of iPSC development is highly appropriate as it opens a window to investigate pre-natal developmental processes in humans *in vitro* and can help to identify early alterations during development in RTT.[14]

Previous studies on iPSC-derived neurons from RTT patients already showed typical neuronal phenotypes, as decreased soma size and reduced number of spines.[15–17] These neurons also presented physiological impairments when compared to iPSC-derived neurons from healthy donors. RTT neurons showed reduced activity and decreased frequency of spontaneous excitatory post synaptic currents. Furthermore, their amplitudes of evoked action potentials were decreased when compared to controls.[17–19] Even though, these studies validated the iPSC-model as a suitable *in vitro* model for RTT, most of the research studies only focussed on the investigation of mature neurons *in vitro*. However, as RTT is a neurodevelopmental disorder this model can also be used to

address and investigate the cause of disease onset.

A more recent study started to investigate developmental processes in iPSC-derived RTT neurons regarding chloride (Cl^-) homeostasis. The findings of that study are in line with findings in mouse models and human *post mortem* tissue, which demonstrate a reduction in the Potassium-chloride-co-transporter 2 (KCC2) causing increased levels of intracellular Cl^-.[10,20–23] KCC2 is expressed in neurons and specific endocrine cells of the pancreas and is responsible for the export of intracellular Cl^-. During early development its expression levels are low, increasing during development.[24] Another important transporter responsible for the import of intracellular Cl^- (Cl^-_i) is the sodium–potassium–chloride-co-transporter 1 (NKCC1). As this transporter is already highly expressed during early development, Cl^-_i is relatively high compared to the extracellular environment. Due to the high Ci^-_i, the neurotransmitter gamma-aminobutyric acid (GABA), usually leading to cellular hyperpolarization in mature cells, has the opposite effect causing depolarizations in immature neurons.[25] During this time period developing neurons show a specific GABA triggered synchronous activity pattern, spontaneous synchronous network activity (SSA), which is essential to trigger further synaptogenesis and form functional networks.[12] This activity is thought to trigger the increase in the expression of KCC2 levels, leading to a reduction of Cl^-_i and thereby triggering the GABAergic shift. This shift is precisely timed and can only be observed for limited duration. In rodents SSA appears mostly within the first two post-natal weeks, while in humans this activity is already abolished at birth.[12,26] As SSA is supposed to have an impact on KCC2 increase, suppression of SSA appearance could potentially lead to a reduction of KCC2, which might change the ratio of KCC2/NKCC1 and therefore, delays or abolishes the GABAergic shift.[27] Interestingly, delays in the GABAergic shift, resulting in an imbalanced E/I, could have already been associated with other neurodevelopmental disorders such as ASD, Angelmann Syndrome or Fragile-X Syndrome.[28–31] Therefore, reduced KCC2 levels presumably caused by insufficient SSA in RTT neurons, could also implement a disturbed GABAergic shift in human neurons, leading to an impaired neuronal maturation with delayed network development.

To investigate if the neuronal alterations in RTT are triggered by an alteration in the GABAergic shift, suggesting an alteration in typical neuronal development, our approach was to study SSA appearance during critical periods of neuronal network maturation in humans.[32] Therefore, we used iPSC derived neurons from RTT patients and controls to investigate activity patterns during neuronal maturation *in vitro*. Our aim was to study GABA triggered SSA in the developing neuros and investigate if neurons lacking functional MeCP2 show a delay in the appearance of this activity. Therefore, our approach was to establish a human *in vitro* model that is capable of investigating and describing functional alterations in early development and which can be used to study alterations in GABAergic shift in human RTT neurons.

RESULTS

GENERATION OF IPSC-DERIVED NEURONS AND MORPHOLOGICAL ANALYSIS BY HIGH CONTENT SCREENING

Before neuronal differentiation was induced, fibroblast-derived iPSCs from RTT patients and healthy controls were characterised for pluripotency by immunocytochemistry (ICC) (Fig. 1A). Afterwards, we induced cortical neurodevelopment by a classical dual SMAD inhibition approach.[33] At neuronal induction day 50, iPSC-derived neurons showed typical neuronal morphology and expression of neuronal markers as MAP2 and SMI312 (Fig. 1B). Development of synapses was confirmed by the co-localisation of VGLUT2 puncta on MAP2 positive dendrites (Fig. 1B i).

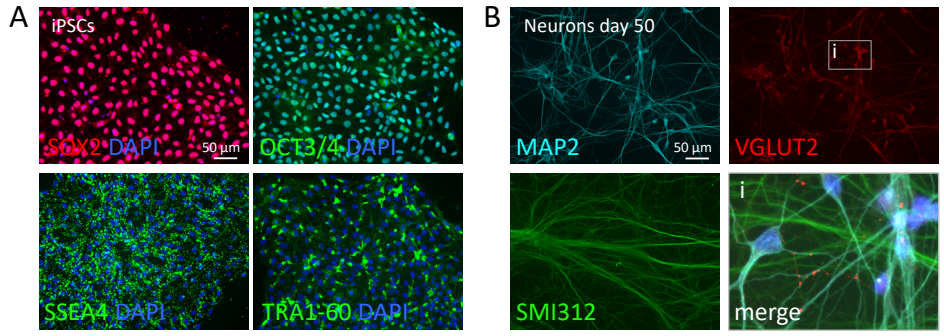

Figure 1. In vitro disease model of Rett Syndrome. *Representative ICC of iPSC line expressing pluripotency markers SOX2, OCT3/4, SSEA4 and TRA1-60 (A). Representative neuronal culture at induction day 50 expressing MAP2, SMI312 and VGLUT2 (B).*

To investigate morphological alterations, we performed high content screening (HCS) analysis on RTT neurons (RTT_del3-4, RTT_T158M, RTT_R255X) and isogenic controls (RTT_del3-4_iso, RTT_T158M_iso) that were generated from the same patient fibroblasts. As we were not capable of generating isogenic controls from patient RTT_R255X in time, we included an additionally control line (CTR_781.5). At day 50 of neuronal differentiation, we analysed changes in total neurite length and axonal segment branching between RTT and control samples by using the automated Columbus imaging software. This analysis revealed a significant decrease in total neurite length in iPSC-derived RTT neurons, based on changed MAP2-positive signal (pixels) per area (Fig. 2A; Mann-Whitney test $p<0.0001$). Furthermore, we analysed axonal segment branching levels by comparing branching points of SMI321 positive segments from RTT neurons to controls.

We detected a reduction in axonal branching in RTT neurons, although this did not reach statistical significance (Fig. 2B; Mann-Whitney test $p=0.12$). Together, we identified alterations in the neuronal phenotype of RTT neurons based on total neurite length at day 50 of neuronal induction.

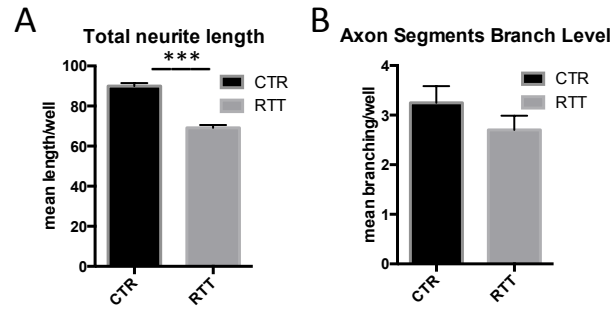

Figure 2. High Content Screening of Neurite Segment Length and Axonal Branching. *HCS results of day 50 neurons from RTT patients and controls on neurite segment length (A) (Mann-Whitney, $p<0.0001$) and axonal branching level (B) (Mann-Whitney, $p=0.12$). Error bars indicate SEM.*

NETWORK DEVELOPMENT AND ACTIVITY IN IPSC DERIVED NEURONS

To investigate network activity of developing neurons in RTT cultures, we performed Ca^{2+}-imaging at different stages of neuronal differentiation (Fig. 3A+B). Every other day during day 33 to day 50 of the protocol, we measured properties of SSA. Therefore, we imaged iPSC-derived neurons from two RTT patients (RTT_R255X and RTT_del3-4), one isogenic control (RTT_del3-4_iso) and one control line (CTR_svu207). In total, we repeated the Ca^{2+}-imaging experiments 4 times for RTT patient and 3 times for control neuron cultures (Fig. 3C-F). In control neurons, we observed a minor increase in SSA frequency up to day 42 of neuronal differentiation, after which SSA activity dropped and stayed low until day 50 (Fig. 3C). In RTT neurons, lower SSA frequencies than in control cultures were initially seen, which stayed low until day 42 of neuronal development. Thereafter, we observed an increase in SSA activity, which reached frequency levels of control neurons measured before day 42 (Fig. 3C). However, alterations in SSA frequency in RTT compared to control neuron cultures did not reach statistical significance (Mann-Whitney test; $p=0.0728$).

To investigate changes in activity levels in individual RTT neurons, we analysed the mean frequency of spikes. In the controls, we observed a higher frequency of spikes when

compared to RTT neurons during the early measurements up to day 45. In comparison, RTT neurons displayed a significant lower mean frequency over the entire measured time period (Fig. 3E; Mann-Whitney test, *p=0.0041*). Based on these findings, we tested whether the number of active cells in RTT cultures changed during the differentiation process. Here, we observed a relatively high and constant number of cells being active in the control neuron cultures from day 35 onwards. In RTT neuron cultures, fewer neurons were active up to day 45 of neuronal differentiation (Fig. 3D; Mann-Whitney test, *p=0.014*). However, from day 45 onwards, the number of active cells in RTT neuron cultures increased and eventually reached activity levels of control neurons.

Further, we investigated whether the relative number of active cells firing synchronously was altered in RTT neuron cultures (Fig. 3F). We measured the number of neurons showing SSA and observed a significant decrease in RTT compared to control neuron cultures (Mann-Whitney test, *p=0.026*). While control neurons showed constant number of cells participating in SSA, which only decreased slightly from day 48 onwards, RTT neurons displayed a significantly lower number of active cells participating in SSA during early recordings. However, this number increased over time and reached control level at day 50. While not all analysis reached statistical significance, the differences observed between RTT and control neurons indicate reduced activity in RTT neuron cultures. Observations suggest a decrease in firing rate of neurons (Fig. 3E) as well as in the ability to fire synchronously (Fig. 3F). Nevertheless, changes observed in individual neuron and SSA activity analysis indicate a recovery in RTT neuron cultures at progressed differentiation stages with a delay of approximately 8 to 10 days in comparison to control neurons (Fig. 3C+D).

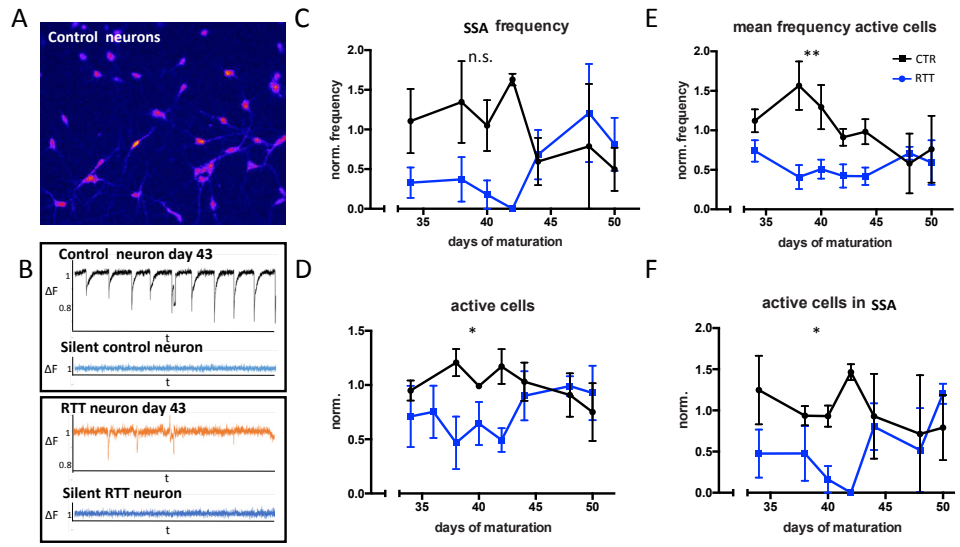

Figure 3. Analysis of Ca^{2+}-imaging. *Field of view analysed during recording (A). Example trace (inverted) of an active and silent control neuron (B, top) and RTT neuron (B, bottom) at differentiation day 43. Normalized frequency of occurring spontaneous synchronous activity (SSA) in RTT neurons compared to controls over time (Mann-Whitney test, p=0.073) (C). Normalized amount of active neurons over time (Mann-Whitney test, p=0.014) (D). Normalized mean frequency of firing rate of individual neurons (Mann-Whitney test, p=0.0041) (E). Normalized amount of active cells firing synchronous in SSA (Mann-Whitney test, p=0.026) (F). Frequencies and numbers of cells were normalized by the mean of controls. Error bars indicate SEM.*

DISCUSSION

To investigate if the lack of functional MeCP2 impairs early neuronal development, we measured changes in neuronal morphologies and addressed changes in Ca^{2+} transients in RTT neuron and control cultures. Our analysis indicated a significant decrease in total neurite length in RTT neurons while alterations in axonal branching were not statistical significant. By Ca^{2+}-imaging analysis, we found a decrease in spontaneous activity in RTT neurons during early maturation. Additionally, RTT neurons showed a significant lower number of cells participating in SSA until day 44 of neuronal differentiation. Interestingly, while mean frequency of active cells stayed lower in RTT neurons, the number of active cells, SSA frequency and number of active cells participating in SSA increased after approximately 8 to 10 days to levels initially observed in control neurons. This finding suggests that the activity patterns in RTT neurons develop at later stages. As SSA is essential for neuronal maturation and synaptogenesis, a delay of this activity might cause impaired neuronal development and lead to a neuronal phenotype common in RTT.

The reduction in total neurite length observed in RTT cultures, are in line with earlier findings, showing impaired neuronal development in RTT patients' brain tissue.[1,34,35] Furthermore, morphological alterations were also described in RTT mouse models.[36–38] Altered dendritic and axonal growth, as well as disturbed axonal guidance and reduced branching in RTT mice are reported. Even though we observed alterations in dendritic growth, we could not show significant alterations of neuronal growth with regards to axonal segment branching. As changes in *in vitro* mouse tissue were observed in performing axonal guidance experiments, similar approaches could be of interest for human neuron cultures.[36] As we investigated axonal segment branching without specifically influencing axonal guidance, the outcome of our study might be different. Furthermore, our neurons were co-cultured with wild type (wt) rat astrocytes to properly mature them. As indicated in previous studies, changes in MeCP2 expression in glia cells is associated with the neuronal phenotype observed in RTT.[39,40] Therefore, axonal growth could be influenced by wt astrocytes, reducing the common RTT phenotype.[41] Nevertheless, in our iPSC-derived model we did observe reduced dendritic length in RTT neurons, suggesting developmental impairments comparable to previous studies.[38] In RTT, morphological alterations in neurons most likely appear during pre-natal development. Alterations observed in previous mouse studies were already identified at post-natal day 2.[38] This early post-natal time point in mice reflects a pre-natal developmental stage in humans.[42–44] It is also known that iPSC-derived neurons reflect an immature neuronal phenotype due to lack of proper ageing *in vitro*.[45,46] We assume that our iPSC-derived RTT model at day 50 of differentiation displays a developmental stage comparable to 7-14 post-natal days in mice, corresponding to the second half of gestation in humans.[42] Therefore, our findings suggests that RTT patients do manifest phenotypic alterations in cortical neurons at early pre-natal stages.

Between day 33 and 50 of neuronal differentiation, we were capable of identifying spontaneous and synchronous Ca^{2+} signals. We specifically looked at the appearance of SSA, a typical activity pattern observed in developing brain areas which also occurs in cortical *in vitro* cultures.[47] As we could not observe these signals before day 33 or after day 50, we defined this period as a critical time window of *in vitro* SSA appearance. Observing neurons over time, RTT neurons showed a constant low activity (Fig. 3E). These findings are in line with a previous study on iPSC-derived RTT neurons, showing a reduction in frequency and amplitude of appearing spontaneous activity.[17] When further looked into synchronous activity in RTT neurons, we observed an initial decrease in active cell number (Fig. 3D) as well as SSA frequency (Fig. 3A) compared to controls. However, both increased after an additional 8-10 days in culture, reaching levels of control samples at day 48 of neuronal induction. Therefore, our findings suggest a delay in SSA appearance in RTT neurons. To study if molecular cascades underlying SSA are affected by lack of MeCP2 and if delayed SSA is comparable to activity observed in controls, further studies are needed. More specifically, it would be necessary to investigate if SSA appearance in RTT neurons follows a similar but simply delayed pattern, or if it appears for a shorter period. To investigate this, the observation time window should be extended. Based on earlier insights in RTT patients, it is expected that alterations during these critical periods of brain development, including delays, can have severe consequences such as development of epilepsy or autism later in life.[48–50] Therefore, we suggest that the here observed alterations might be the origin of observed functional impairments in RTT.

Previous studies have shown that SSA is an essential trigger for KCC2 expression and synaptogenesis. Interestingly, we and other researchers identified a reduction in KCC2 expression levels in iPSC-derived RTT neurons and *post mortem* tissue from RTT patients (Chapter 2).[11,21,23,25] Therefore, targeting KCC2 expression could be an option to correct for a potential inefficient SSA and to normalize maturation defects in RTT neurons. Earlier studies targeted NKCC1 by using the diuretic bumetanide, an NKCC1 inhibitor, to regulate Cl^-homeostasis in neurons.[51–55] In clinical trial, bumetanide reduced number of severe seizures in Autism Spectrum Disorder (ASD) patients, who already presented typical symptoms.[53] Therefore, studying this approach on patients, including RTT patients, before clinical symptoms manifest could be attractive. By decreasing Cl^-_i in neurons during or

only shortly after a critical time window, insufficient SSA could be compensated for, thereby supporting network connectivity and maturation. By timing this approach during early life, long-term consequences might be prevented and RTT symptoms could be reduced or even abolished. This approach would clearly need further validation. Nevertheless, with our findings we introduce an iPSC-based model system, which is capable to detect alterations in early network development, setting a basis for follow up studies.

MATERIAL METHODS

CELL CULTURE

Reprogramming and iPSC culturing

Rett patient Fibroblasts were obtained from the *Cell lines and DNA bank of Rett Syndrome, X-linked mental retardation and other genetic disease*, member of the Telethon Network of Genetic Biobanks. Three patient lines carrying different mutation within *MECP2* were cultured showing a deletion within exon 3 and 4 (RTT-FB DEL), carrying a nonsense mutation p.R255X (RTT-FB R225X) or showing a missense mutation at p.T158M (RTT-FB T158M). Control Fibroblasts were received from two anonymous healthy males (CTR-FB svu207, CTR-FB 781.5). All lines were cultured and expanded in Fibroblast medium (DMEM-F12, 20% FBS, 1%NEAA, 1%Pen/Strep, 50 µM β-Mercaptoethanol). The generation of pure RTT-fibroblasts and isogenic controls was performed for RTT-FB T158M and RTT-FB DEL as described before.[56] In brief, single fibroblasts were plated in wells of a 96-well plate and cultured for expansion. Created fibroblasts lines were tested on MeCP2 expression by immunohistochemistry and PCR. Only pure MeCP2 positive or negative fibroblast lines were further expanded for iPSCs generation.[57] For RTT-FB R225X only pure negative fibroblast line could be generated due to extreme X-chromosomal skewing. To reprogram fibroblasts towards iPSCs, 4x10^5 fibroblasts were resuspended in 400 µl Gene Pulser® Electroporation Buffer Reagent (BioRad) containing 23.3 µg of each of three plasmids (Addgene, Plasmid #27078, #27080, #27076). Cells were then electroporated with Gene Pulser II (BioRad), giving three pulses of 1.6 kV, 3 µF and 400 Ω resistance. Cells were plated on Geltrex® (A14132-02, ThermoFisher) coated plates and left to recover overnight in Fibroblast medium without antibiotics but containing 10 µM ROCK-inhibitor (Y-27632). After 24 h medium was changed to Fibroblast medium including Penicillin/Streptavidin and cells were further cultured until they reached 60-70% confluence. Then medium was changed to TeSR™-E7™ (Stemcell Technologies) and refreshed daily. iPSC colonies appeared after 21-28 days and were manually picked and further cultured on Vitronectin XF™ coated plates in TeSR™-E8™ (Stemcell Technologies) as described before.[56]

Neuronal differentiation

Neuronal differentiation was performed as published before with minor adjustments.[33] In brief, iPSCs were cultured in high density in TeSR™-E8™. Medium was switched to Neuro maintenance medium (NMM) containing 1 µM Dorsomorphin and 10 µM SB431 and replaced daily. Neuronal rosette structures appeared and were manually picked after 10-12 days. These were expanded on Polyornithine/Laminin coated plates in NMM containing 20 ng/ml FGF-2 and 20 ng/ml EGF. When cells reached 90% confluence,

medium was changed to N2-medium containing 400 ng/ml of human SHH and changed daily for four days. Afterwards, cells were treated with 10 µM valproic acid in neurobasal medium (NB). To mature neurons, they were plated on primary rat astrocytes and grown in NB containing BDNF, GDNF and cAMP up to 56 days.

IPSC AND NEURONAL CHARACTERISATION

Embryoid Body formation

To validate ability of iPSCs to generate all three germ layers and therefore be pluripotent, iPSCs were detached from cell culture plate and transferred to anti adhesive Poly(2-hydroxyethyl methacrylate) (Sigma-Aldrich) coated wells of a 6-well plate. Cells were cultured floating in TeSR™-E8™ (STEMCELL) with 10 µM ROCK-inhibitor (Y-27632) for 48h with half of medium being changed daily. From day 3 medium was changed to TeSR™-E8™ without ROCK-inhibitor and EBs were cultured up to day 10. At day 10 EBs were plated on Geltrex®-coated coverslips and further cultured in TeSR™-E8™ for another three days. Afterwards cells were fixated and prepared for immunocytochemistry (ICC).

Immunocytochemistry

Cells of interest were washed with PBS and fixated with 4% PFA for 10 min at RT. After 3x washes with PBS cells were blocked and permeabilized for 1 h in blocking- buffer (PBS, 5% normal goat serum (Gibco®), 0.1% bovine serum albumin (Sigma-Aldrich), 0.3% Triton X-100 (Sigma-Aldrich)). Primary antibodies (Tab. 1) were diluted in blocking buffer and cells were incubated with antibody solution for 1 h at RT followed by an overnight incubation at 4°C. Next day cells were washed 3x with PBS for 10 min and secondary antibodies Alexa Fluor® 488/594/647 (ThermoFisher, 1:1000, mo, rb, gp, ch) in blocking buffer were applied and incubated for 1-2 h at RT. Afterwards DAPI was stained for 5 min in PBS and cells were washed 3x with PBS again before coverslips were mounted with Fluoromount™ (Sigma-Aldrich) on glass slides.

HIGH CONTENT SCREENING

Day 50 neurons from RTT iPSC lines (RTT_del3-4, RTT_T158M, RTT_R255X), two isogenic contro lines (RTT_del3-4_iso, RTT_T158M_iso) and one healthy control line (CTR_781.5), plated on 96-well glass bottom plates, were fixated and stained as described above. Afterwards, 20 wells per line were scanned by the Opera confocal microscope and images were analysed for neurite segment length and axonal branching by using the Columbus Image Data Storage and Analysis System (PerkinElmer).

Table 1. Primary Antibodies for ICC and IHC

Antibody	Manufacturer	Host	Dilution
MeCP2	CellSignalling	rb	1:200
OCT4	Santa Cruz	mo	1:1000
SSEA4	DSHB	mo	1:50
TRA1-60	Santa Cruz	mo	1:200
TRA1-81	Millipore	mo	1:250
SOX2	Millipore	rb	1:1000
ß-III Tubulin	R&D Systems	mo	1:1000
α-Fetoprotein	R&D Systems	mo	1:1000
α-Smooth Muscle Actin	Progene	mo	1:1000
MAP2	Abcam	ch	1:500
SMI312	Eurogentec	mo	1:1000
VGLUT2	SYnaptic SYstems	rb	1:1000
VGLUT1	SYnaptic SYstems	rb	1:250
VGAT	SYnaptic SYstems	gp	1:500

CA^{2+}- IMAGING

Ca^{2+}-Imaging was performed at different days of the neuronal induction of iPSCs starting with day 33. Measurements were repeated every two to three days until neuronal induction day 50. Two RTT lines (RTT_del3-4, RTT_R255X), one isogenic control line (RTT_del3-4_iso) and one healthy control line (CTR_svu207) was analysed. Therefore, neurons plated and cultivated on glass coverslips were incubated with 2mM of Fluo-5F AM (ThermoFisher) for 5 min at 37°C. Afterwards neurons were washed once with Neurobasal medium (ThermoFisher) and directly processed for imaging. Glass coverslips were placed into imaging chamber of a Nikon confocal microscope and superfused with 37°C ACSF (127mM NaCl, 25mM NaHCO3, 25mM D-glucose, 2.5 mM KCl, 1mM MgCl2, 2mM CaCl2, 1.25mM NaH2PO4) equilibrated with 95% O_2 and 5% CO_2. Recordings of the neurons were made at 1.6 Hz for 8 min and analysis performed by using Event Analyser (EvA) in MatLab (Mathworks) as described before.[58]

STATISTICS

To compare different lines and experiments properly, all data points were divided by the average of control measurements before statistical analysis. All statistical analysis and calculations were performed with Graphpad Prism 6. Data sets were tested for normal distribution and statistical test chosen accordingly. Therefore, Mann-Whitney test was chosen to compare axon segment branching level, neurite segment length and neuronal activity, measured by Ca^{2+}-imaging in control and RTT neurons. Significant differences were considered when $p<0.05$.

AUTHORS CONTRIBUTION

LH was responsible for cell culture including iPSC generation, characterization and neuronal differentiation. LH also performed immunocytochemistry and HCS. Ca^{2+}-Imaging was performed by LH and JDP. MatLab analysis was implemented by JP. RM and VMH supervised planning of experiments and writing of the manuscript.

REFERENCES

1. Armstrong, D. D. Rett syndrome neuropathology review 2000. *Brain Dev.* **23**, 72–76 (2001).
2. Jellinger, K., Seitelberger, F. & Armstrong, D. D. Neuropathology of Rett Syndrome. *J. Child Neurol.* **20**, 747–753 (2005).
3. Ip, J. P. K., Mellios, N. & Sur, M. Rett syndrome: Insights into genetic, molecular and circuit mechanisms. *Nat. Rev. Neurosci.* **19**, 368–382 (2018).
4. Amir, R. E. *et al.* Rett syndrome is caused by mutations in X-linked MECP2 , encoding methyl-CpG-binding protein 2. *Nat. Genet.* **23**, 185–188 (1999).
5. Gabel, H. W. *et al.* Disruption of DNA-methylation-dependent long gene repression in Rett syndrome. *Nature* (2015). doi:10.1038/nature14319
6. Chao, H.-T., Zoghbi, H. Y. & Rosenmund, C. MeCP2 controls excitatory synaptic strength by regulating glutamatergic synapse number. *Neuron* **56**, 58–65 (2007).
7. Dani, V. S. *et al.* Reduced cortical activity due to a shift in the balance between excitation and inhibition in a mouse model of Rett syndrome. *Proc. Natl. Acad. Sci. U. S. A.* **102**, 12560–5 (2005).
8. Moretti, P. *et al.* Learning and memory and synaptic plasticity are impaired in a mouse model of Rett syndrome. *J. Neurosci.* **26**, 319–27 (2006).
9. Guy, J., Gan, J., Selfridge, J., Cobb, S. & Bird, A. Reversal of neurological defects in a mouse model of Rett syndrome. *Science* **315**, 1143–1147 (2007).
10. Banerjee, A. *et al.* Jointly reduced inhibition and excitation underlies circuit-wide changes in cortical processing in Rett syndrome. *Proc. Natl. Acad. Sci. U. S. A.* **113**, E7287–E7296 (2016).
11. Lozovaya, N. *et al.* Early alterations in a mouse model of Rett syndrome: the GABA developmental shift is abolished at birth. *Sci. Rep.* **9**, 9276 (2019).
12. Ben-Ari, Y., Gaiarsa, J.-L., Tyzio, R. & Khazipov, R. GABA: A Pioneer Transmitter That Excites Immature Neurons and Generates Primitive Oscillations. *Physiol. Rev.* **87**, 1215–1284 (2007).
13. Williams, L. A., Davis-Dusenbery, B. N. & Eggan, K. C. SnapShot: Directed Differentiation of Pluripotent Stem Cells. *Cell* **149**, 1174-1174.e1 (2012).
14. Zhu, Z. & Huangfu, D. Human pluripotent stem cells: an emerging model in developmental biology. *Development* **140**, 705–17 (2013).
15. Kim, K.-Y., Hysolli, E. & Park, I.-H. Neuronal maturation defect in induced pluripotent stem cells from patients with Rett syndrome. *Proc. Natl. Acad. Sci.* **108**, 14169–14174 (2011).
16. Ananiev, G., Williams, E. C., Li, H. & Chang, Q. Isogenic pairs of wild type and mutant induced pluripotent stem cell (iPSC) lines from Rett syndrome patients as in vitro disease model. *PLoS One* **6**, e25255 (2011).
17. Marchetto, M. C. N. *et al.* A model for neural development and treatment of Rett syndrome using human induced pluripotent stem cells. *Cell* **143**, 527–39 (2010).
18. Chin, E. W. M. *et al.* Choline Ameliorates Disease Phenotypes in Human iPSC Models of Rett Syndrome. *NeuroMolecular Med.* **18**, 364–377 (2016).
19. Djuric, U. *et al.* MECP2e1 isoform mutation affects the form and function of neurons derived from Rett

syndrome patient iPS cells. *Neurobiol. Dis.* **76**, 37–45 (2015).

20. Tang, X. *et al.* KCC2 rescues functional deficits in human neurons derived from patients with Rett syndrome. *Proc. Natl. Acad. Sci. U. S. A.* 1524013113- (2016). doi:10.1073/pnas.1524013113
21. Gogliotti, R. G. *et al.* Total RNA Sequencing of Rett Syndrome Autopsy Samples Identifies the M4 Muscarinic Receptor as a Novel Therapeutic Target. *J. Pharmacol. Exp. Ther.* **365**, 291–300 (2018).
22. Duarte, S. T. *et al.* Abnormal Expression of Cerebrospinal Fluid Cation Chloride Cotransporters in Patients with Rett Syndrome. *PLoS One* **8**, 1–7 (2013).
23. Hinz, L., Torrella Barrufet, J. & Heine, V. M. KCC2 expression levels are reduced in post mortem brain tissue of Rett syndrome patients. *Acta Neuropathol. Commun.* **7**, 196 (2019).
24. Kovács, K., Basu, K., Rouiller, I. & Sík, A. Regional differences in the expression of K+-Cl- 2 cotransporter in the developing rat cortex. *Brain Struct. Funct.* **219**, 527–538 (2014).
25. Ben-Ari, Y. Excitatory actions of gaba during development: the nature of the nurture. *Nat Rev Neurosci* **3**, 728–739 (2002).
26. Khazipov, R. *et al.* Early development of neuronal activity in the primate hippocampus in utero. *J. Neurosci.* **21**, 9770–9781 (2001).
27. Hübner, C. A. *et al.* Disruption of KCC2 reveals an essential role of K-Cl cotransport already in early synaptic inhibition. *Neuron* **30**, 515–24 (2001).
28. Harada, M. *et al.* Non-Invasive Evaluation of the GABAergic/Glutamatergic System in Autistic Patients Observed by MEGA-Editing Proton MR Spectroscopy Using a Clinical 3 Tesla Instrument. *J. Autism Dev. Disord.* **41**, 447–454 (2011).
29. Sinkkonen, S. T., Homanics, G. E. & Korpi, E. R. Mouse models of Angelman syndrome, a neurodevelopmental disorder, display different brain regional GABA(A) receptor alterations. *Neurosci. Lett.* **340**, 205–8 (2003).
30. Gibson, J. R., Bartley, A. F., Hays, S. A. & Huber, K. M. Imbalance of neocortical excitation and inhibition and altered UP states reflect network hyperexcitability in the mouse model of fragile X syndrome. *J. Neurophysiol.* **100**, 2615–26 (2008).
31. Tyzio, R. *et al.* Oxytocin-Mediated GABA Inhibition During Delivery Attenuates Autism Pathogenesis in Rodent Offspring. *Science (80-.).* **343**, 675–679 (2014).
32. Kasyanov, A. M., Safiulina, V. F., Voronin, L. L. & Cherubini, E. GABA-mediated giant depolarizing potentials as coincidence detectors for enhancing synaptic efficacy in the developing hippocampus. *Proc. Natl. Acad. Sci. U. S. A.* **101**, (2004).
33. Nadadhur, A. G. *et al.* Multi-level characterization of balanced inhibitory-excitatory cortical neuron network derived from human pluripotent stem cells. *PLoS One* **12**, 1–21 (2017).
34. Armstrong, D., Dunn, J. K., Antalffy, B. & Trivedi, R. Selective dendritic alterations in the cortex of Rett syndrome. *J. Neuropathol. Exp. Neurol.* **54**, 195–201 (1995).
35. Jellinger, K. & Seitelberger, F. Neuropathology of Rett syndrome. *Am. J. Med. Genet. Suppl.* **1**, 259–88 (1986).
36. Degano, A. L., Pasterkamp, R. J. & Ronnett, G. V. MeCP2 deficiency disrupts axonal guidance, fasciculation, and targeting by altering Semaphorin 3F function. *Mol. Cell. Neurosci.* **42**, 243–54 (2009).
37. Belichenko, P. V. *et al.* Widespread changes in dendritic and axonal morphology in Mecp2-mutant mouse models of Rett syndrome: Evidence for disruption of neuronal networks. *J. Comp. Neurol.* **514**, 240–258 (2009).
38. Baj, G., Patrizio, A., Montalbano, A., Sciancalepore, M. & Tongiorgi, E. Developmental and maintenance defects in Rett syndrome neurons identified by a new mouse staging system in vitro. *Front. Cell. Neurosci.* **8**, (2014).
39. Gonzalez, D. M., Gregory, J. & Brennand, K. J. The Importance of Non-neuronal Cell Types in hiPSC-Based Disease Modeling and Drug Screening. *Front. Cell Dev. Biol.* **5**, 1–14 (2017).
40. Williams, E. C. *et al.* Mutant astrocytes differentiated from Rett syndrome patients-specific iPSCs have adverse effects on wildtype neurons. *Hum. Mol. Genet.* **23**, 2968–2980 (2014).
41. Rigby, M. J., Gomez, T. M. & Puglielli, L. Glial Cell-Axonal Growth Cone Interactions in Neurodevelopment and Regeneration. *Front. Neurosci.* **14**, 203 (2020).
42. Pressler, R. & Auvin, S. Comparison of brain maturation among species: An example in translational research suggesting the possible use of bumetanide in newborn. *Front. Neurol.* **4 APR**, 1 (2013).
43. Workman, A. D., Charvet, C. J., Clancy, B., Darlington, R. B. & Finlay, B. L. Modeling transformations of neurodevelopmental sequences across mammalian species. *J. Neurosci.* **33**, 7368–7383 (2013).
44. Semple, B. D., Blomgren, K., Gimlin, K., Ferriero, D. M. & Noble-Haeusslein, L. J. Brain development in rodents and humans: Identifying benchmarks of maturation and vulnerability to injury across species. *Prog. Neurobiol.* **106–107**, 1–16 (2013).
45. Studer, L., Vera, E. & Cornacchia, D. Programming and Reprogramming Cellular Age in the Era of Induced Pluripotency. *Cell Stem Cell* **16**, 591–600 (2015).
46. Mariani, J. *et al.* Modeling human cortical development in vitro using induced pluripotent stem cells. *Proc. Natl. Acad. Sci. U. S. A.* **109**, 12770–5 (2012).
47. Opitz, T., De Lima, A. D. & Voigt, T. Spontaneous Development of Synchronous Oscillatory Activity During Maturation of Cortical Networks In Vitro. *J. Neurophysiol.* **88**, 2196–2206 (2002).
48. Kozol, R. A. Prenatal neuropathologies in autism spectrum disorder and intellectual disability: The gestation of a comprehensive Zebrafish model. *J. Dev. Biol.* **6**, (2018).
49. Park, S. H. *et al.* Tuberous sclerosis in a 20-week gestation fetus: Immunohistochemical study. *Acta Neuropathol.* **94**, 180–186 (1997).
50. W, K., S, K. & HJ, L. Electrical Activity Patterns and the Functional Maturation of the Neocortex. *Eur. J. Neurosci.* **34**, (2011).
51. Tyzio, R. *et al.* Oxytocin-mediated GABA inhibition during delivery attenuates autism pathogenesis in rodent offspring. *Science (80-.).* **343**, 675–679 (2014).
52. Ben-Ari, Y., Damier, P. & Lemonnier, E. Failure of the Nemo Trial: Bumetanide Is a Promising Agent to Treat Many Brain Disorders but Not Newborn Seizures. *Front. Cell. Neurosci.* **10**, 1–6 (2016).
53. Lemonnier, E. *et al.* A randomised controlled trial of bumetanide in the treatment of autism in children. *Transl. Psychiatry* **2**, e202 (2012).
54. Hu, J.-J. *et al.* Bumetanide reduce the seizure susceptibility induced by pentylenetetrazol via inhibition of aberrant hippocampal neurogenesis in neonatal rats after hypoxia-ischemia. *Brain Res. Bull.* **130**, 188–199

(2017).

55. Dzhala, V. I., Brumback, A. C. & Staley, K. J. Bumetanide enhances phenobarbital efficacy in a neonatal seizure model. *Ann. Neurol.* **63**, 222–35 (2008).

56. Hinz, L., Hoekstra, S. D., Watanabe, K., Posthuma, D. & Heine, V. M. Generation of Isogenic Controls for In Vitro Disease Modelling of X-Chromosomal Disorders. *Stem Cell Rev. Reports* 1–10 (2018). doi:10.1007/s12015-018-9851-8

57. Okita, K. *et al.* A more efficient method to generate integration-free human iPS cells. *Nat. Methods* **8**, 409–412 (2011).

58. Hjorth, J. J. J. *et al.* Detection of silent cells, synchronization and modulatory activity in developing cellular networks. *Dev. Neurobiol.* **76**, 357–374 (2016).